# Application of Induced Polarization and Resistivity Methods to Identify Subsurface Layers in Bauxite Deposits Area of Kendawangan, West Kalimantan

## Muhardi*, M. Anwar, Kaharudin

Department of Geophysics, Universitas Tanjungpura Pontianak, Indonesia

**Abstract**

Kendawangan Sub-district, Ketapang Regency is one of the areas in West Kalimantan Province containing minerals of economic value, namely bauxite deposits. This study has applied both induced polarization and resistivity methods. It aims to identify subsurface layers in the Kendawangan bauxite deposit area based on resistivity and chargeability distribution. Measurements in the field apply a north-south line using the dipole-dipole configuration, have a length of 144 m, and electrode distance of 3 m. The results showed that the subsurface layer in the study area identified the presence of bauxite deposits. In addition, it showed that the subsurface layers were topsoil, bauxite deposits, saprolite, and bedrock. Topsoil has a thickness of about 1 m, and it is a product of the weathering process. The bauxite deposit has a thickness of about 9 m, and it contains the minerals aluminum oxide, quartz, hematite, and titanium oxide. Saprolite has a thickness of about 2 - 4 m, and it contains aluminum silica (kaolinite) and minerals quartz, titanium oxide, zircon, and it is a weathering product of bedrock. The bedrock is at a depth of more than 10 m, which is interpreted as volcanic tuff, sandstone, and claystone.

## INTRODUCTION

Indonesia has bauxite reserves to rank the 8th largest in the world (Haryadi, 2016). Kendawangan Sub-district, Ketapang Regency is one of the areas in West Kalimantan Province that can contain minerals of economic value, including bauxite deposits, iron ore (Andriansyah, 2019), heavy minerals both of zircon and cassiterite (Setyanto & Surachman, 2017), and radioactive minerals (Subiantoro, Soetopo and Haryanto, 2012). In West Kalimantan, bauxite is found in a distribution line with a length of 300 km and a width

*Correspondence Address:
Jl. Prof. Dr. Hadari Nawawi, Bansir Laut, Pontianak Tenggara, Kota Pontianak, Indonesia, 78124
E-mail: muhardi@physics.untan.ac.id

of 50-100 km (laterite zone), which stretches northwest to southeast from Ketapang Regency, Sanggau, Landak, Kubu Raya, Pontianak, Bengkayang, and Singkawang (Toreno & Moe'tamar, 2012). Therefore, it is necessary to conduct a more effective and efficient survey to identify the presence of bauxite deposits. The results of this study can be used as information to exploit bauxite in the Kendawangan area.

Bauxite is a mineral-containing material composed of aluminum oxide in boehmite ore ($Al_2O_3H_2O$) and gibbsite minerals ($Al_2O_3.3H_2O$) (Husaini, Cahyono and Damayanti, 2014). In general, bauxite contains about 45 - 65% aluminium oxide ($Al_2O_3$), about 1 - 12% Silica ($SiO_2$), about 2 - 25% Hematite ($Fe_2O_3$), more than 3% Titanium Oxide ($TiO_2$), and about 14 - 36% Water ($H_2O$) (Karno et al., 2012). Bauxite is formed from sedimentary rocks with high Al and low both Fe and

quartz ($SiO_2$). Generally, bauxite is formed from syenite, clays, or shale, which has weathered with the dissolution of Na, K, Mg, and Ca into alumina hydroxide (Al(OH)) residue and solidify to bauxite deposits through a dehydration process (Toreno & Moe'tamar, 2012).

Geologically, the Kendawangan area and its surroundings are in the formations of Kerabai Volcanic Rocks (Kuk), Sukadana Granite (Kus), and Alluvium (Qa), as shown in Figure 1. Kerabai volcanic rocks are composed of lithic tuff, crystal tuff, and lava, interbedded with metasandstone, metasiltstone, and metaclaystone. This unit is of Late Cretaceous age. Sukadana granite is composed of granite, granodiorite, and diorite (Sudana, Djamal, & Sukido, 1994). This unit breaks through and crushes the Kerabai Volcano Rocks (Subiantoro et al., 2012). The alluvium is composed of clay, sand, pebble, and cobble. This unit form is the river and coastal deposits (Sudana, et al., 1994).
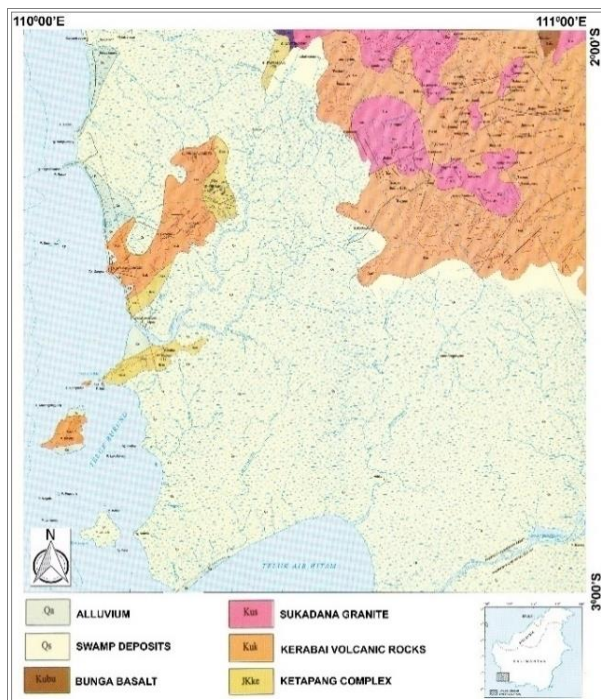


**Figure 1**. Geological Map of Kendawangan (Sudana et al., 1994)

Induced polarization (IP) is an active method by injecting an electric current into the earth's subsurface. When the electric current stops being injected, so the voltage should change to zero (Everett, 2013). However, it will store electrical energy like a capacitor and then be released in specific media. Even though the current has stopped, the voltage will decay with time and gradually disappear (Everett, 2013). The method has often been used, for example, to observe the distribution of iron ore ((Ferial, Natalisanto, and Lazar, 2019), gold mineralization zones (Yuniarto, 2020), and soil corrosivity (Dewi, Utama, and Rochman, 2017).

The induced polarization is inseparable from the electrochemical and electronic mechanisms of ions in the rock body. Two main influences cause polarization in rock bodies. They are membrane polarization (it is found in sedimentary rocks that do not contain metal) and electrode polarization or overvoltage (it is found when there are metal minerals in rock pores) (Milsom, 2003). Polarization effects can also be seen in rocks containing clay minerals with a negative charge (Everett, 2013).

One method of measuring induced polarization is the time-domain method, which compares the polarized potential to the initial potential injected (Kingman, Ritchie and Rowston, 2019). The physical parameter to be produced is chargeability. It is the ability of rocks to store electric current.
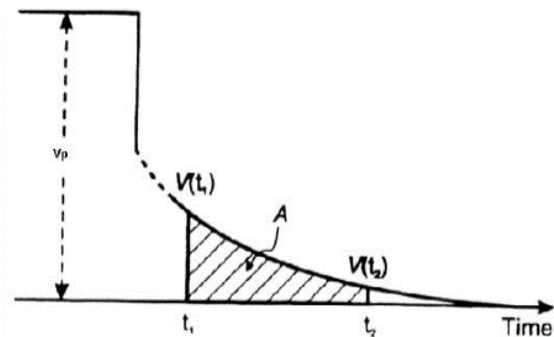


**Figure 2.** The residual voltage is the change in voltage that decays with time, and it makes an area of A (Everett, 2013).

From the response of the polarization graph, can be obtained the value $V_s$, namely the voltage after polarization. It is the result of voltage decay with time, and it results in an area under the

voltage decay curve (Figure 2). Therefore, chargeability can also be reviewed by applying the concept of integral to the value of the voltage after the current is turned off. Apparent chargeability will be obtained with the unit of time, which is formulated in Equation (1).

$$m = \frac{1}{V_p} \int_{t1}^{t2} V_s(t)dt = \frac{A}{V_p} \qquad (1)$$

Where $V_s$ is the potential after the current is turned off at times $t_1$ to $t_2$ and $V_p$ is the initial potential injected (Telford et al., 1990).

The resistivity of a medium is a parameter that shows the medium's ability to inhibit the flow of electric current through the medium's body (Everett, 2013). Thus, a material with higher resistivity means more difficult for electric current to pass (Dentith & Mudge, 2014). This method is often used to identify subsurface conditions, for example, estimation of bauxite distribution (Bolaji et al., 2019; Tira, Arman and Putra, 2015), subsurface layers lithology (Muhardi & Wahyudi, 2019), aquifer layers lithology (Jufriadi & Ayu, 2019), the presence of groundwater (Muhardi, Perdhana and Nasharuddin, 2019), the potential for landslides (Muhardi & Wahyudi, 2020), and the thickness of the peat layer (Muliadi, Zulfian and Muhardi, 2019).

The geoelectric method principle utilizes the injection of currents flowing into the subsurface layers (Everett, 2013). The current flow that passes through the subsurface layer will be used as a reference to identify the material's resistivity value in the layer in which it passes (Everett, 2013). The current flow illustration is shown in Figure 3.
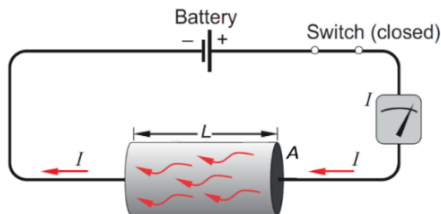


**Figure 3**. Illustration of an electric current flowing in a cylindrical medium (Dentith & Mudge, 2014)

If the electric current *I* flowing in a medium is cylindrical with length *L* and surface area *A*, then the resistivity value of the medium can be formulated by Equation (2) (Everett, 2013).

$$\rho = R \frac{A}{L} \qquad (2)$$

Where *R* is the medium resistance which is influenced by the geometry of the medium.

## METHOD

The study area was conducted in the Kendawangan area, Ketapang Regency. Chargeability and resistivity measurements are applied with a line from point A in coordinates 2°25'40.21"S and 110°9'28.15"E to point A' in coordinates 2°25'44.93"S and 110°9'27.82"E. The survey equipment used is an automatic resistivity system (ARES) 12 Volt, current and potential electrodes, accumulator, and cables. The measuring line has a north-south direction have a length of 144 m, as shown in Figure 4. The distance between the electrodes is 3 m to identify the subsurface layer with a 1 m or more depth.
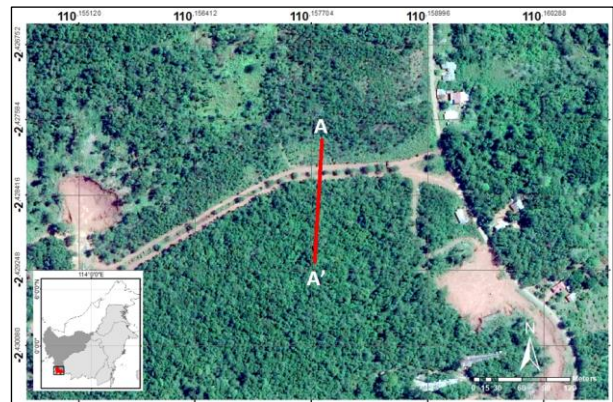


**Figure 4.** The survey design on the study area

In this study, a dipole-dipole configuration is used because it is considered the most effective to produce variations in the chargeability and resistivity values of rocks at a depth. The subsurface layer will be described (Dewi, et al., 2017). These two methods are generally used to describe the subsurface layer (Amaya, Dahlin, Barmen, & Rosberg, 2016).

The geoelectric instrument used in field measurements is the Automatic Resistivity and IP System (ARES). The electrode arrangement of the dipole-dipole configuration can be seen in Figure 5. In general, two current electrodes and two potential electrodes are used. The distance between the

electrodes is the same, namely *a*. This configuration has a ratio factor of *n*. The more significant the ratio factor, the deeper the depth of chargeability value that will be interpreted.
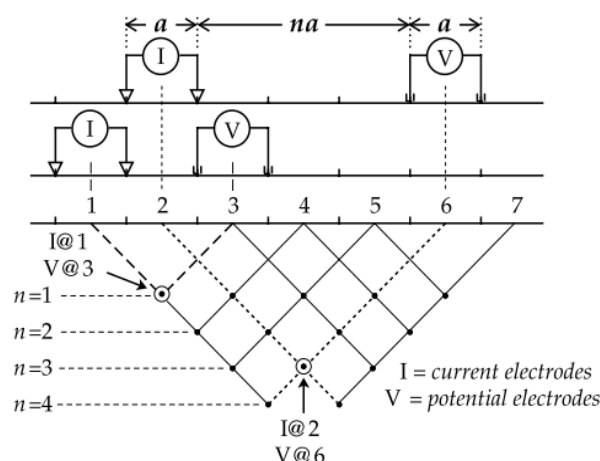


**Figure 5**. Illustration of dipole-dipole configuration in IP and resistivity methods (Everett, 2013)

The data processing aims to obtain the distribution of chargeability and resistivity from observations and calculations. Then the inversion process is carried out using the Res2Dinv software so that a 2D cross-section of chargeability and resistivity is obtained according to field conditions. The next step is to interpret the subsurface layer by referring to field conditions, geological maps, chargeability, and resistivity. The amount of chargeability will indicate whether the polarization effect has long disappeared after the current is turned off. The chargeability of various materials is presented in Table 1. The resistivity value obtained is used as a reference to identify subsurface layers (Nogueira et al., 2011). They are bauxite deposits, bedrock, and other layers in the study area. The resistivity value is interpreted based on the approach in Table 2.

**Table 1.** The chargeability of various materials (Telford et al., 1990)

| Materials | Chargeability (msec) |
|---|---|
| 20% Sulfides | 2,000 – 3,000 |
| 8 – 20 % Sulfides | 1,000 – 2,000 |
| 2 – 8 % Sulfides | 500 – 1,000 |
| Volcanic tuffs | 300 – 800 |
| Sandstone, siltstone | 100 – 500 |

| | |
|---|---|
| Shale | 50 – 100 |
| Granite, grandodiorite | 10 – 50 |
| Limestone, dolomite | 10 – 20 |

**Table 2.** The resistivity of minerals and rock types (Telford et al., 1990); Milsom, 2003)

| Mineral and rock types | Resistivity ($\Omega$m) |
|---|---|
| Bauxite | $2\times10^2 – 6\times10^3$ |
| Hematite | $3.5\times10^{-3} – 10^7$ |
| Magnetite | $5\times10^{-5} – 5.7\times10^3$ |
| Biotite | $2\times10^2 – 10^6$ |
| Gabbro | $10^3 – 10^6$ |
| Quartz | $4\times10^{10} – 2\times10^{14}$ |
| Basalt | $10 – 1.3\times10^7$ |
| Clays | $1 – 10^2$ |
| Granite | $4.5\times10^3 – 1.3\times10^6$ |
| Limestones | $50 – 10^7$ |
| Andesite | $1.7\times10^2 – 4.5\times10^4$ |
| Tuffs | $2\times10^3 - 10^5$ |
| Lavas | $10^2 – 5\times10^4$ |
| Dolomite | $3.5\times10^2 – 5\times10^3$ |
| Sandstones | $1 – 6.4\times10^8$ |
| Shale | $20 – 2\times10^3$ |
| Topsoil | $50 – 100$ |

## RESULT AND DISCUSSION

The study applies a north-south line with a long 141 m, and spacing between electrodes is 3 m. Based on the inversion process results, a 2D cross-section with a range of resistivity values is 331 - 118.947 $\Omega$m, as shown in Figure 6a. Also, a range of chargeability values is 24.1 - 699 msec, as shown in Figure 6b. They are spread to a depth of 17.9 m. These two sections are used as references for interpreting the layers around the bauxite deposit. They are weathered layers and bedrock. Interpretation also refers to field conditions to estimate the layer thickness in the study area.

Based on the two sections, the resistivity distribution shows layers that can be interpreted as topsoil, bauxite deposit, saprolite layer, and bedrock (Syahruna, 2019). It also refers to rock conditions in the field, as shown in Figure 7. Meanwhile, the chargeability distribution shows a higher value at a line distance of 117 – 123 m with

a depth of 5 – 13 m. Bauxite deposit is a layer that contains metallic minerals, so it has a higher chargeability value when compared to topsoil or the layer above it. However, this chargeability cross-section does not show the boundary between layers because there is no clear contrast. This layer with a high chargeability value is assumed to be bedrock which is interpreted as volcanic tuff.

The volcanic tuff shows a higher chargeability anomaly when compared to the surrounding layers (Dentith & Mudge, 2014). This high chargeability value indicates a long decay time and suggests the presence of conductive minerals (Everett, 2013). Besides, based on the resistivity value, bedrock is also composed of sandstones and claystones. These rocks will have weathering (laterization process), which is thought to have occurred due to igneous rock (granite) intrusion, resulting in bauxite deposits (Toreno & Moe'tamar, 2012). Bauxite is formed from weathering sedimentary rocks with high Al and low both Fe and quartz ($SiO_2$).



(a)



(b)
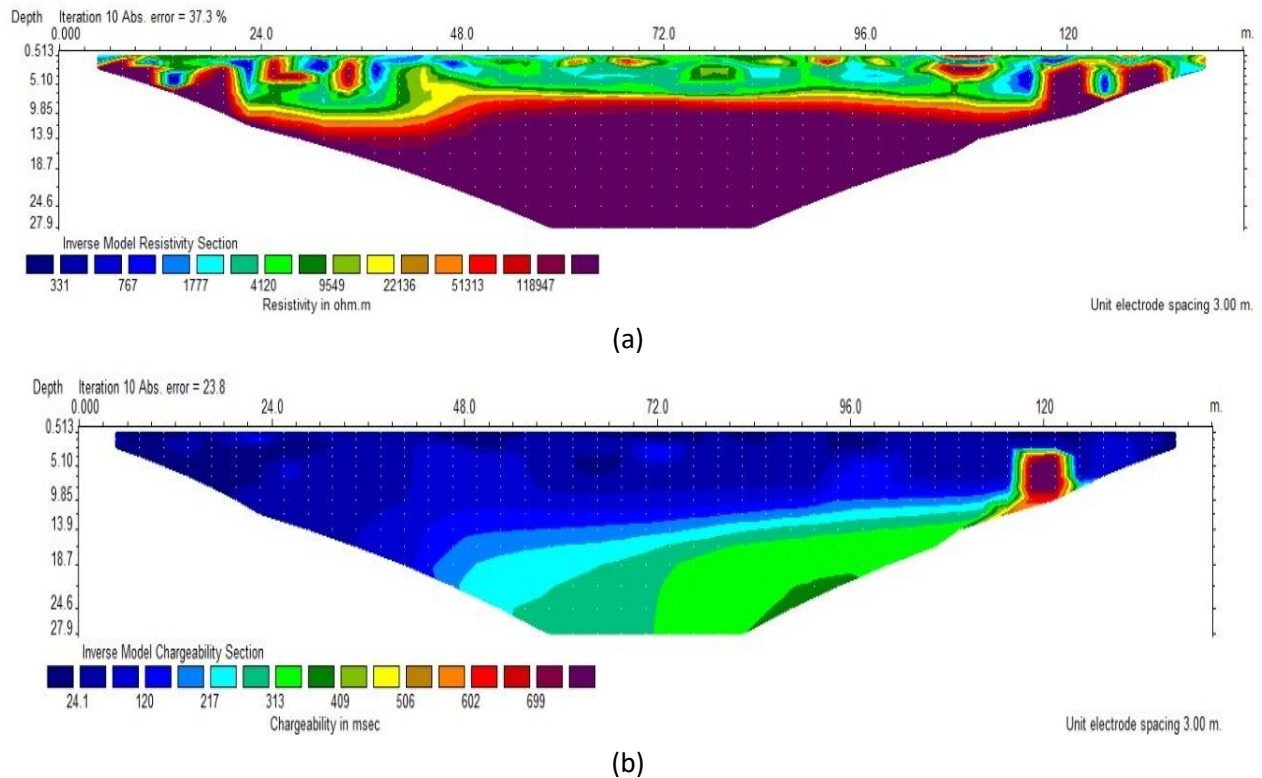
**Figure 6.** 2D cross-section both of resistivity distribution (a) and chargeability distribution (b)



**Figure 7.** The bauxite deposits in the study area that has been exploited

Interpretation result of 2D cross-section based on resistivity distribution in the study area as shown in Figure 8a, and based on chargeability distribution as shown in Figure 8b. Following the 2D resistivity and chargeability sections, geological maps, and conditions in the field, the top layer is interpreted as topsoil, a product of the weathering process (physics and chemistry) of the layer below it. In this study, the topsoil was not detected by the resistivity or chargeability section because its thickness is approximately 1 m. The electrode spacing of 3 m is thought to be less able to detect the relatively shallow top layer, but field observations indicate this topsoil's presence.



(a)



(b)
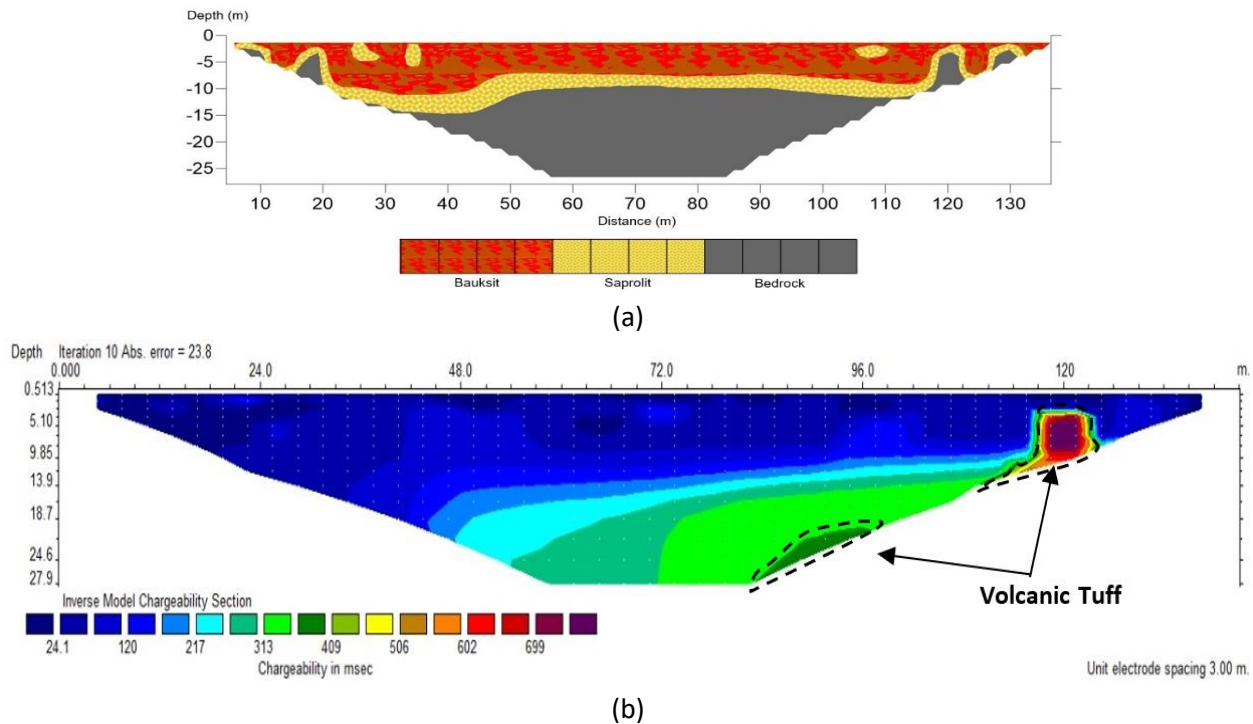
**Figure 8**. Interpretation result of 2D cross-section based on both resistivity distribution (a) and chargeability distribution (b)

There are several layers below the topsoil. First, bauxite deposits with a resistivity value of 331 - 4120 Ωm (Bolaji et al., 2019), containing aluminum oxide, quartz, hematite, and titanium oxide minerals (Karno et al., 2012). The bauxite layer is scattered along the measurement line but is dominant at a distance of about 21 - 117 m with a thickness of about 9 m. Second, the layer under the bauxite deposit is saprolite with a resistivity value above 4120 Ωm and a thickness of about 2 - 4 m. Saprolite contains aluminum silica (kaolinite) and the minerals quartz, titanium oxide, zircon (Syahruna, 2019). It is a weathering product of bedrock. Saprolite is generally lighter in color than the bauxite deposits above it, with a brownish-orange, whitish orange, and reddish. Third, bedrock with a

resistivity value above 118,947 Ωm is interpreted as volcanic tuff, sandstones, and clays and is at a depth of more than 10 m. Based on the chargeability cross-section, the bedrock, which is interpreted as volcanic tuff, can also be identified with a value range of 409 - 699 msec.

## CONCLUSION

The study results showed that the subsurface layer identified the presence of bauxite deposits in the study area. In addition, it showed that the subsurface layers were topsoil, bauxite deposits, saprolite, and bedrock. Topsoil has a thickness of about 1 m and is a product of the weathering process. The bauxite deposit has a

thickness of about 9 m, containing the minerals aluminum oxide, quartz, hematite, and titanium oxide. Saprolite has a thickness of about 2 - 4 m, contains aluminum silica (kaolinite) and quartz minerals, titanium oxide, zircon. It is a weathering product of bedrock. The bedrock is at a depth of more than 10 m, which is interpreted as volcanic tuff, sandstone, and claystone.

## REFERENCES

Amaya, A. G., Dahlin, T., Barmen, G., & Rosberg, J. E. (2016). Electrical Resistivity Tomography and Induced Polarization for Mapping the Subsurface of Alluvial Fans: A Case Study in Punata (Bolivia). *Geosciences (Switzerland)*, *6*(4), 1-13. http://dx.doi.org/10.3390/geosciences6040051.

Andriansyah, R. (2019). Model Genesa Endapan Besi di Kecamatan Kendawangan, Ketapang, Kalimantan Barat. *Journal of Applied Science (JAPPS)*, *1*(2), 41–49. https://doi.org/10.36870/japps.v1i2.51.

Bolaji, E. A., Lawrence, A. O., Akindele, O., Femi, A. O., Ayoola, O. R., Ojo, T. A., & Amos, O. O. (2019). Geoelectric Assessments of the Bauxite Ore Deposit at Orin_Ekiti, Southwestern Nigeria. *International Journal of Applied Environmental Sciences*, *14*(2), 197–210. Retrieved at https://www.ripublication.com/ijaes19/ijaesv14n2_06.pdf.

Dentith, M., & Mudge, S. (2014). *Geophysics for the Mineral Exploration Geoscientist*. Cambridge : Cambridge University Press.

Dewi, K. K., Utama, W., & Rochman, J. P. G. N. (2017). Pemetaan Zona Korosivitas Tanah Berdasarkan Nilai Chargeability Menggunakan Metode Time Domain Induced Polarization Konfigurasi Dipole-Dipole Studi Kasus PT. IPMOMI. *Jurnal Geosaintek*, *3*(2), 137–142. http://dx.doi.org/10.12962/j25023659.v3i2.2971.

Everett, M. E. (2013). *Near-Surface Applied Geophysics*. Cambridge University Press.

Ferial, D., Natalisanto, A. I., & Lazar, P. A. (2019). Identifikasi Sebaran Mineral Bijih Besi dengan Menggunakan Metode Resistivitas dan Induced (IP) di Kecamatan Muara Uya, Kabupaten Tabalong, Provinsi Kalimantan Selatan. *Jurnal Geosains Kutai Basin*, *2*(2), 1–9. Retrieved at http://jurnal.fmipa.unmul.ac.id/index.php/geofis/article/view/471.

Haryadi, H. (2016). Analisis Lost Opportunity (LO) Bauksit Indonesia. *Jurnal Teknologi Mineral Dan Batubara*, *12*(1), 45–57. http://dx.doi.org/10.30556/jtmb.Vol12.No1.2016.230.

Husaini, Cahyono, S. S., & Damayanti, R. (2014). Upgrading of Tayan'S Crude Bauxite Using Rotary Drum Scrubber. *Indonesian Mining Journal*, *17*(1), 40–52. https://doi.org/10.30556/imj.Vol17.No1.2014.343.

Jufriadi, A. & Ayu, H. D. (2019). Underground Water-Level Monitoring by Integrated Study of Geoelectric, Logging, Cutting and Pumping Data in Industrial Area of Candi Sub-District, Sidoarjo. *Jurnal Pendidikan Fisika Indonesia*, *15*(2), 122–128. https://doi.org/10.15294/jpfi.v15i2.14365.

Karno, W., Syahrial, E., Falahti, A., Napitupulu, A. T., Darmawan, A., & Kurniasih, T. N. (2012). *Kajian Kebijakan Pengembangan Industri Mineral Sebagai Kawasan Ekonomi Khusus*. Jakarta : Pusat Data dan Informasi Energi dan Sumber Daya Mineral, Kementerian Energi dan Sumber Daya Mineral.

Kingman, J. E. E., Ritchie, T. J., & Rowston, P. (2019). Induced Polarization Chargeability Calibration Standards. *ASEG Extended Abstracts*, 1–5. http://dx.doi.org/10.1080/22020586.2019.12073143.

Milsom, J. (2003). *Field Geophysics* (3rd ed.). New York : John Wiley and Sons.

Muhardi, Perdhana, R., & Nasharuddin. (2019). Identifikasi Keberadaan Air Tanah Menggunakan Metode Geolistrik Resistivitas Konfigurasi Schlumberger (Studi Kasus: Desa Clapar Kabupaten Banjarnegara). *Prisma Fisika*, *7*(3), 331–336. http://dx.doi.org/10.26418/pf.v7i3.39441.

Muhardi, & Wahyudi. (2019). Identifikasi Litologi Area Rawan Longsor di Desa Clapar-Banjarnegara Menggunakan Metode Geolistrik Resistivitas Konfigurasi Schlumberger. *Jurnal Fisika*, *9*(2), 52–59. http://dx.doi.org/10.15294/jf.v9i2.21409.

Muhardi, & Wahyudi. (2020). Prediksi Tipe Longsor di Desa Clapar Menggunakan Metode Geolistrik Resistivitas Konfigurasi Dipol-dipol. *Jurnal Lingkungan dan Bencana Geologi*, *11*(2), 115–123. http://dx.doi.org/10.34126/jlbg.v11i2.290.

Muliadi, Zulfian, & Muhardi. (2019). Identifikasi Ketebalan Tanah Gambut Berdasarkan Nilai Resistivitas 3D: Studi Kasus Daerah Tempat Pembuangan Akhir Batu Layang Kota Pontianak. *Positron*, *9*(2), 86–94. http://dx.doi.org/10.26418/positron.v9i2.34821.

Nogueira, P. V., Rocha, M. P., Borges, W. R., Cunha, L. S. Da, Seimetz, E. X., Cavalcanti, M. M., & Azevedo, P. A. De. (2011). Use of Seismic Refraction and Resistivity in Bauxite Deposit in the Region of Barro Alto – Goiás, Brazil. *Proceedings of Twelfth International Congress of the Brazilian Geophysical Society*. Rio de Janeiro, Brazil : Société Géologique de France.

Setyanto, A., & Surachman, M. (2017). The Occurences of Heavy Mineral Placer at Kendawangan and Its Surrounding, West Kalimantan Province. *Bulletin of the Marine Geology*, *32*(1), 33–40.

Subiantoro, L., Soetopo, B., & Haryanto, D. (2012). Kajian Awal Prospek Bahan Galian Monasit di Kendawangan Kalimantan Barat. *Eksplorium*, *33*(2), 97–110.

http://dx.doi.org/10.17146/eksplorium.2012.33.2.2660

Sudana, D., Djamal, B., & Sukido. (1994). *Geological Map of the Kendawangan Quadrangle, Kalimantan.* Bandung : Pusat Penelitian dan Pengembangan Geologi.

Syahruna, C. F. (2019). *Pemodelan Zonasi Endapan Bauksit Laterit di Daerah Air Upas Kecamatan Ketapang, Provinsi Kalimantan Barat* (Unpublished Undergrade Thesis). Universitas Trisakti, Jakarta.

Telford, W. M., Geldart, L. P., & Sheriff, R. E. (1990). *Applied Geophysics* (2nd Ed.). Cambridge : Cambridge University Press.

Tira, H., Arman, Y., & Putra, Y. S. (2015). Pendugaan Sebaran Kandungan Bauksit dengan Metode Geolistrik Konfigurasi Schlumberger di Desa Sungai Batu Kabupaten Sanggau Kalimantan Barat. *Positron*, *5*(2), 58–64. http://dx.doi.org/10.26418/positron.v5i2.12018.

Toreno, E. Y., & Moe'tamar. (2012). Karakteristik Cebakan Bauksit Laterit di Daerah Sepiluk - Senaning, Kabupaten Sintang, Kalimantan Barat. *Buletin Sumber Daya Geologi*, *7*(2), 45–56. https://doi.org/10.47599/bsdg.v7i2.102.

Yuniarto, A. H. P. (2020). Aplikasi Time Domain Induced Polarization dalam Eksplorasi Emas di Blok "CPY" Gunung Pongkor Kabupaten Bogor. *Jurnal Geosaintek*, *6*(3), 117–126. http://dx.doi.org/10.12962/j25023659.v6i3.6867.